SIMULATION MODELS OF BUILDING INTEGRATED COLLECTORS AND PV MODULES

Kanade Hirayanagi[1], Mitsuhiro Udagawa[1], Yasuyo Matoba[1], Takafumi Kusunoki[1]

Makoto Satoh[2] and Hyun-woo Roh[3]

[1] Department of Architecture, Kogakuin University, Tokyo (Japan)

[2] Satoh Energy Research Co., Ltd, Tokyo (Japan) [3] OM Solar Co., Ltd, Shizuoka (Japan)

1. Introduction

In recent years, as the solar collectors and PV modules are often integrated into building envelopes, it is necessary to develop the simulation models for these solar components. For the integrated collectors, reduction of heat loss to the outside air is expected from the collector backside comparing to the roof mounted collectors using frames. Contrarily, the efficiency of the power generation by the PV modules is reduced due to higher temperature with thermal insulation effect on the backside of the PV modules. In addition, the building integrated solar collectors and PV modules effect the thermal properties of the roof and exterior walls as the building components. In this study, the simulation models of roof integrated solar collector including PV module are described. The simulation of a whole solar heating system with the integrated solar collectors with PV modules was carried out to evaluate the solar heat collection, the generated electricity by PV modules, reductions of space heating and domestic hot water heating loads.

2. Collectors and PV modules

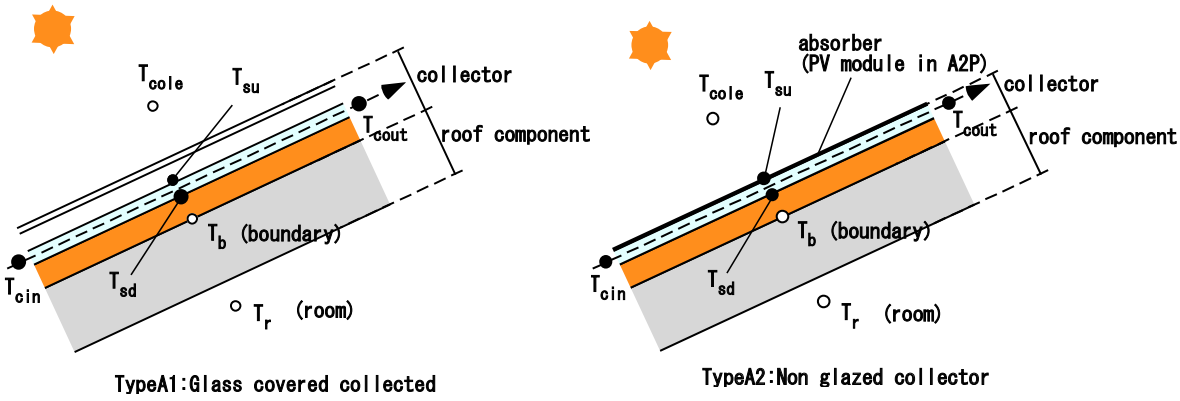

Fig. 1 Simulation model of solar collectors

Fig. 1 shows three types of air solar collector.Type A1 is a glass covered collector, Type A2 is a non-glazed collector and Type A2P is a non-glazed collector with PV modules. The calculation models for both collectors are composed of the upper collector part and the lower roof component. Type A1 uses one glass cover and the absorber plate is painted in black. Type A2 is a model without glass cover, same as Type A1 the absorber is painted in black. Type A2P is the same as Type A2 except for the PV modules being used as the absorber(PVT collector). For the solar collector part the steady state heat transfer model to calculate the collected heat considering the temperature of the roof component. For the roof component, unsteady state heat conduction model is used using the boundary condition considering the solar collector. In the study to calculated the parameters shown in Tab. 2, the roof-integrated solar collectors, the solar collector and the roof were connected using the boundary temperature, T_b. Tab. 1. shows the equations for calculating thermal performance of solar collectors. Where T_{cole} is a environmental temperature for the integrated collectors calculated from outer environmental temperature T_{coleu} and inner environmental temperature T_{coled} as shown in Tab. 1.

Tab. 1 Parameters for calculating thermal performance of solar collectors

	K_{su}	K_{sd}	K_c	T_{coleu}	T_{coled}	SG	T_{cole}
TypeA1 Glass covered collector	$\frac{1}{r_a + 1/\alpha_o}$	$\frac{1}{r_b + 1/\alpha_{ox}}$	$K_{cu} + K_{cd}$	$\frac{SG}{K_{su}} - \frac{R_{skyc}}{\alpha_o} + T_o$	T_b	$(\tau_g a_s I)_e$	$k_u T_{coleu} + k_d T_{coled}$
TypeA2 Non glazed collector	α_o	$\frac{1}{r_b + 1/\alpha_{ox}}$	$K_{cu} + K_{cd}$	$\frac{SG}{K_{su}} - \frac{R_{skyc}}{\alpha_o} + T_o$	T_b	$(a_s I)_e$	$k_u T_{coleu} + k_d T_{coled}$
TypeA2P PVT collector	α_o	$\frac{1}{r_b + 1/\alpha_{ox}}$	$K_{cu} + K_{cd}$	$\frac{SG}{K_{su}} - \frac{R_{skyc}}{\alpha_o} + T_o$	T_b	$(a_s I - \eta_{pvo} I)_e$	$k_u T_{coleu} + k_d T_{coled}$

K_{su} : upper heat loss coefficient [W/m^{2}K], K_{sd} : lower heat loss coefficient [W/m^{2}K], K_c : heat transmission coefficient [W/m^{2}K]
T_{coleu} : outer environmental temperature [°C], T_{coled} : inner environmental temperature [°C], T_{cole} : environmental temperature [°C]
r_a : thermal resistance of air space [m^{2}K/W], r_b : thermal resistance of backside [m^{2}K/W]
α_o : outside heat transfer coefficient [W/m^{2}K], α_{ox} : backside heat transfer coefficient [W/m^{2}K]
K_{cu} : upper thermal transmittance [W/m^{2}K], K_{cd} : lower thermal transmittance [W/m^{2}K], R_{skyc} : nocturnal radiation [W/m^2]
T_o : outside temperature [°C], T_b : boundary temperature [°C], τ_g : glass cover transmittance [-], a_s : solar radiation absorptivity [-]
I : solar radiation on collector [W/m^2], η_{pvo} : power generation efficiency [-], k_u : upper environmental temperature coefficient [-]
k_d : lower environmental temperature coefficient [-]

Eq. 1 shows the relationship between inlet and outlet temperature, T_{fi} and T_{fo}.

$$T_{fo} = T_{cole} - (T_{cole} - T_{fi}) e^{-\frac{K_c A_c}{CG}} \quad \text{(eq. 1)}$$

Where, T_{cole} is a environmental temperature. K_c is a heat transmission coefficient for the integrated collectors calculated from K_{cu} and K_{cd} in Tab. 1. C and G are the specific heat of air [J/kg.K] and the air flow rate [kg/s], respectively. A_c is the collector area [m^2]

$$E = K_{pv}(T_{pv}) I_{col} A_{su} / I_s \quad \text{(eq. 2)}$$

The power generation of PV array E [W] is calculated based on JIS C8907:2005 as shown in Eq. 1. Where, $K_{pv}(T_{pv})$ is a coefficient expressing the effects of PV cell temperature, T_{pv}. T_{pv} is calculated using the heat balace equation of the upper part of Type A2P collector. I_s is solar radiation on PV array at the standard test condition (1000W/m^2).

Fig. 2 shows the heat collection efficiencies obtained for the typical solar collectors. Tab. 2 shows the solar collector parameters required to simulate the whole system model. The parameters, *tra*, K_{su}, K_{sd}, f_{cu}, f_{cd} were used to run the simulation program EESLISM for the whole system simulation such as Fig. 4.

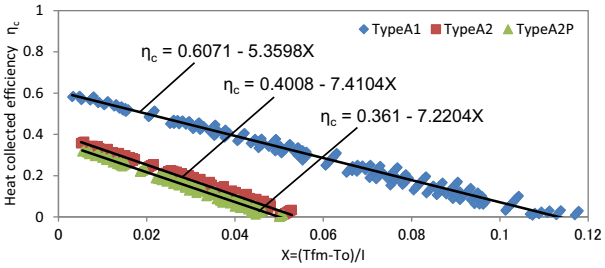

Fig. 2 Heat collection efficiency

Tab. 2 Solar collector parameters

Parameter			TypeA1	TypeA2	TypeA2P
Transmittance × absorptance	tra	[-]	0.86	0.95	0.90
Upper heat loss coefficient	Ksu	[W/m^{2}K]	6.28	16.37	15.93
Lower heat loss coefficient	Ksd	[W/m^{2}K]	0.74	0.74	0.74
Upper efficiency coefficient	fcu	[-]	0.72	0.50	0.50
Lower efficiency coefficient	fcd	[-]	0.86	0.80	0.81

3. Simulation

Fig. 3 shows the floor plan of the simulation model house. Fig. 4 shows the simulation model. Tab. 3 shows the insulation specifications. Tab. 4 shows the simulation cases. Tab. 5 shows the simulation schedule. Simulation model house is a one storied wooden house with a total fioor area of 81.6m^2.The roof tilted angle was varied at the middle of the south roof. The upper roof tilted angle is 38^o. The lower roof tilted angle is 21^o. The solar heating rooms are Living, Aroom and Broom. The Solar collectors are installed on the upper roof and the lower roof. The upper roof collector area is 16.2m^2. The lower roof collector area is 32.3m^2. In this simulation study, four cases was carried out as shown in Tab 4. Case1 is the house without using the solar collector. Cases 2, 3 and 4 were simulated using PV modules and solar collectors.The upper roof collector is glass covered collector in all cases. In Case 2,the non glazed collector without PV module is installed on the lower roof for pre heating.

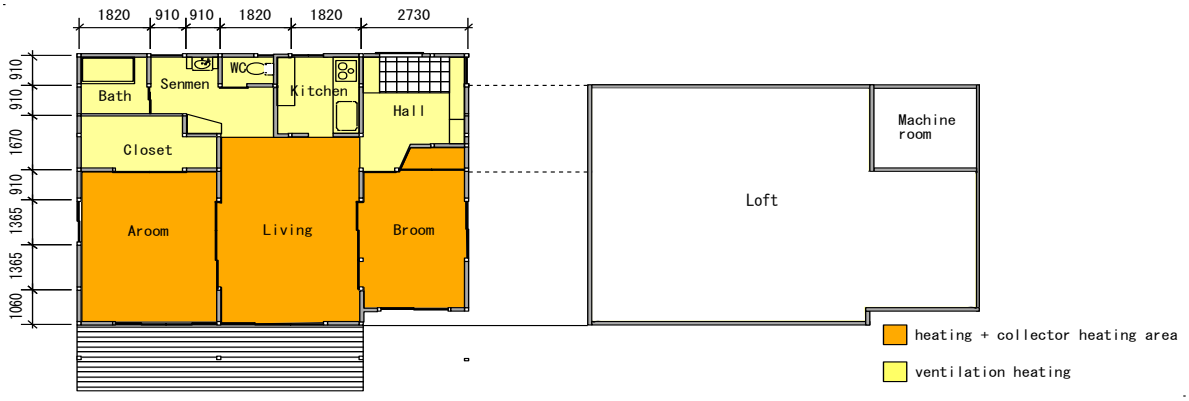

Fig. 3 Floor plan of the simulation model house

Tab. 3 Insulation specifications

	Insulation	
Roof	Glass wool	200 [mm]
	Phenolic foam	60 [mm]
Outside wall	Glass wool	100 [mm]
	Phenolic foam	35 [mm]
Floor	polystyrene foam	30 [mm]
Windows	Low-e, double pane U=2.08 W/m^{2}K	6 + 6 [mm]

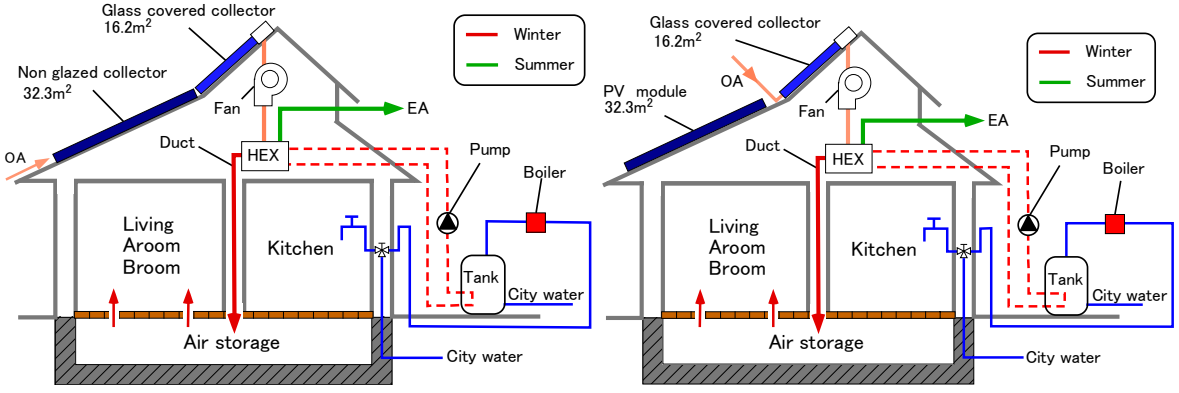

Case2 and 4 **Case3**

Fig. 4 Simulation model house

Tab. 4 Simulation Case

	Solar collector					
	Preheat collector and/or PV module			Heat collector		
	Lower roof	Type	Area[m^2]	Upper roof	Type	Area[m^2]
Case1	-	-	-	-	-	-
Case2	Non glazed collector	Type A2	32.3	Glass covered collector	Type A1	16.2
Case3	PV module	-	32.3	Glass covered collector	Type A1	16.2
Case4	PVT collector	Type A2P	32.3	Glass covered collector	Type A1	16.2

Tab. 5 Simulation schedule

Weather data		Expanded AMeDAS(Maebashi)
Simulation period		Jan.-Mar. Nov.-Dec.
Calculation interval		1 hour
Room set point control		Operative temperature 18°C
Room temperature control time	Living	6:00 - 14:00 17:00 - 23:00
	Aroom	6:00 - 7:00 19:00 - 23:00
	Broom	6:00 - 7:00 19:00 - 23:00
Collector tilted angle	Upper	38°
	Lower	21°
Collector azimuth angle		0°
Start collector fan		Surface Temperature 40°C
Flow rate		570m^3/h
Solar heating rooms		Living, Aroom, Broom

In Case 3, the PV module is installed simply on the lower roof. Therefore, there is no pre-heat collection in Case 3. The lower roof is used only for power generation. Therefore, the heat collection is only in the upper roof glazed collector. In Case 4 the PVT collector is installed on the lower roof for the power generation as well as pre-heating.

The solar collector fan was started when the collector absorber surface temperature was over 40°C. The solar collector flow rate was 570m^3/h. The rooms Living, Aroom and Broom were heated in winter by the hot air from the under floor heat storage as shown in Fig 4. In winter, the heat exchanger for DHW heating is used when the Living air temperature exceeds 28°C. In summer, the collected heat used to heat the water for DHW. The weather data of Maebashi of the expanded AMeDAS was used. The simulation interval is 60 minutes.

4. Simulation results

Fig. 5 shows the weather data for the winter typical days. Fig. 6 shows the simulation results of Case 1. Fig. 7 shows the simulation results of Case 2. Fig.8 shows the simulation results of Case 3. Fig. 9 shows the simulation results of Case 4.
The solar radiation in Cases 2 and 4 reached about 35kW on the sunny day with 48.5m^2 of the collector area. In Case 3, the solar collector is used only on the upper roof. The solar radiation in Case3 reached about 15kW on the sunny days with 16.2m^2 of the collector area.

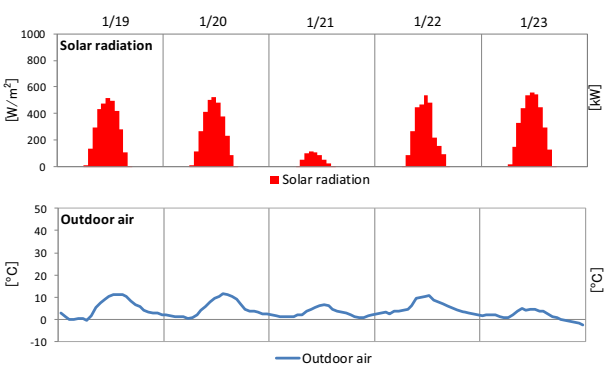

Fig. 5 Weather data on winter

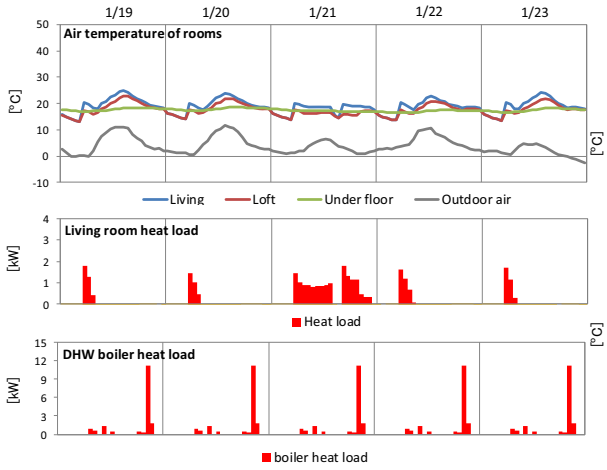

Fig. 6 simulation results of Case1

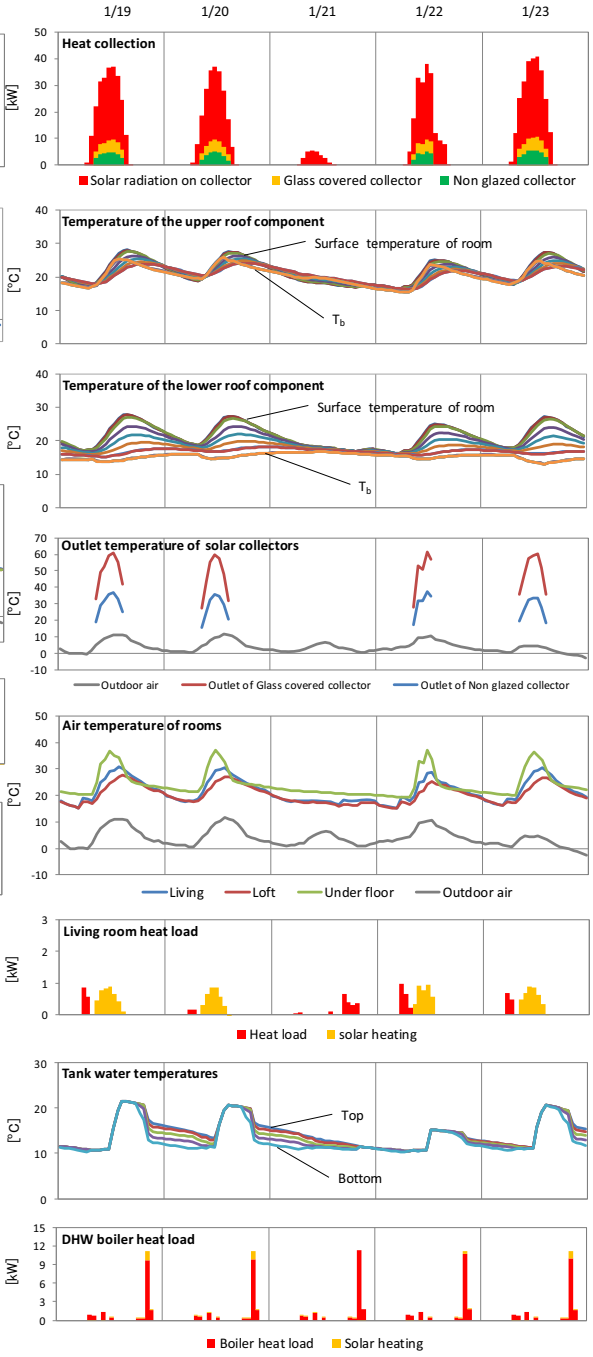

Fig. 7 simulation results of Case2 (Non glazed collector)

The heat collection in Cases 2 and 4 was reached about 10kW for the total of the upper roof collector and the lower roof collector. However, the heat collection in Case 3 is 5kW. Case 3 is different because the heat collection on the only upper roof. Cases 2 and 4, there was no significant difference in the heat collection. The maximum power generation is about 2kW for Cases 3 and 4. There was little difference by the cases. Therefore, it would not be large difference in the cell temperature due to the PV module cooling effect on the backside. The outlet air temperatures of the lower roof solar collector in Cases 2 and 4 reached about 30°C. The outlet air temperatures of the upper roof solar collector in Cases 2 and 4 reached over 50°C.

Therefore, the boundary temperature T_b was low in comparison with the roof inside surface temperature. The PV surface temperature in Cases 3 reached about 35°C. The PV surface temperature in Case 4 was 33°C at the maximum. The temperature difference of the two Cases was very small and only small effect on increasing PV power generation by PVT collector. The outlet air temperature of upper roof solar collector in Case 3 reached about 40°C. Therefore, the boundary temperature T_b did not rise. However, because in Cases 2 and 4 the roof is well insulated, the influence of the collector for the rooms was small. The room temperatures rose high in Cases 2, 3 and 4 compared with Case 1. The Living air temperatures in Cases 2, 3 and 4 reached about 30°C by solar heating. The underfloor heat storage in Cases 2 and 4 reached about 35°C by solar heating. However, the underfloor heat storage in Case 3 reached about 30°C.

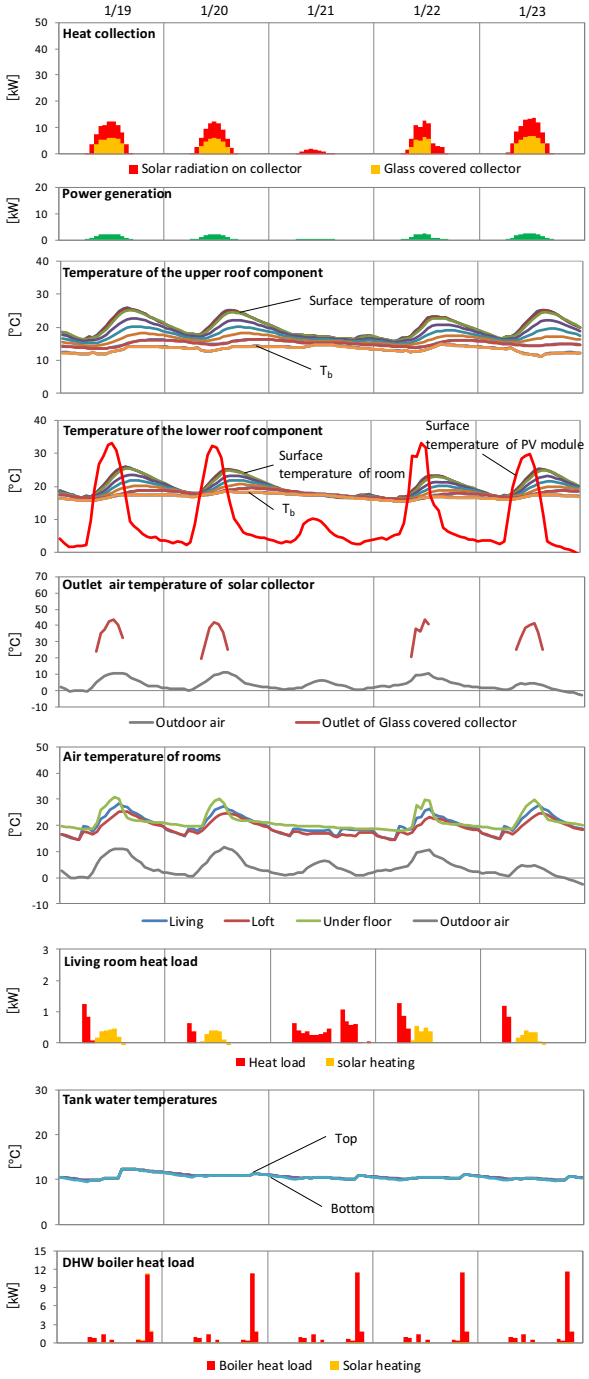

Fig. 8 simulation results of Case3 (PV module without pre-heat collector)

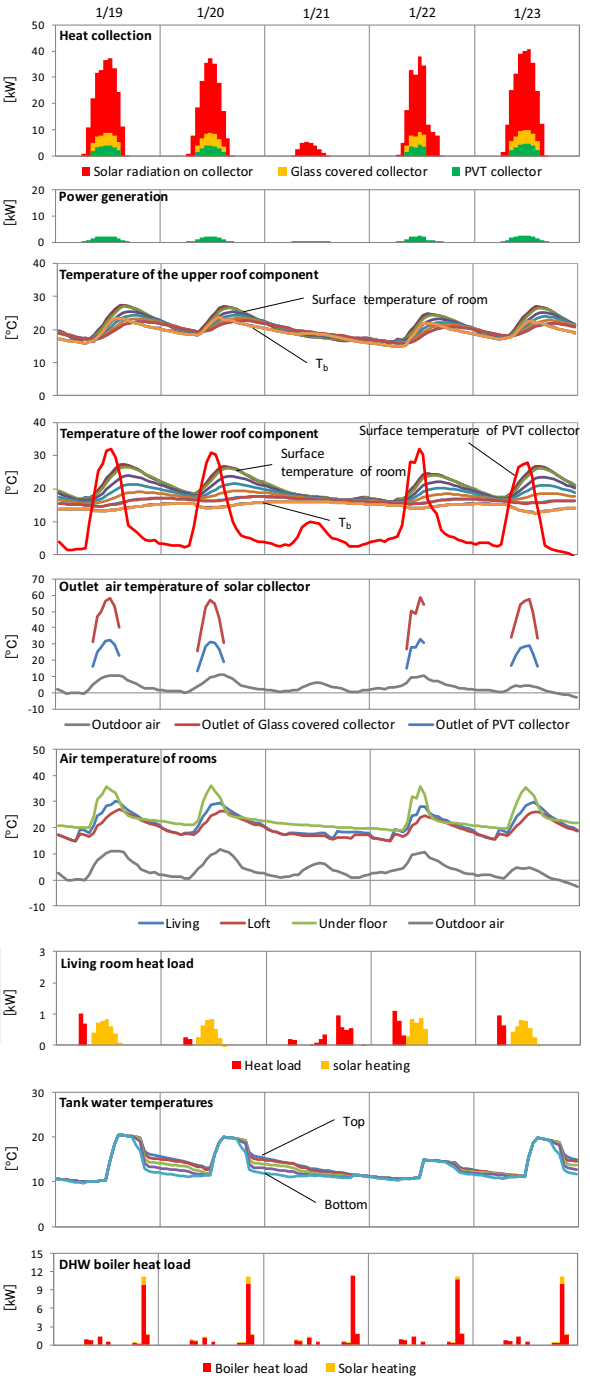

Fig. 9 simulation results of Case4 (PVT collector)

The Loft air temperature did not change substantially in all Cases. The solar heating in Cases 2 and 4 reached about 1kW on the sunny day. The solar heating in Case 3 reached about 0.3kW on the sunny day. The heat load in the morning decreased in Cases 2 and 4 on the cloudy day. The indoor room conditions were almost same for Cases 2, 3 and 4.The tank water temperature in Cases 2 and 4 reached about 55°C. The tank water temperature in Case3 reached about 45°C. The tank water temperature in Cases 2 and 4 reached about 55°C on the sunny day. The boiler heat load in Cases 2 and 4 reached about 5kW. The boiler heat load in Case 3 reached about 3kW.

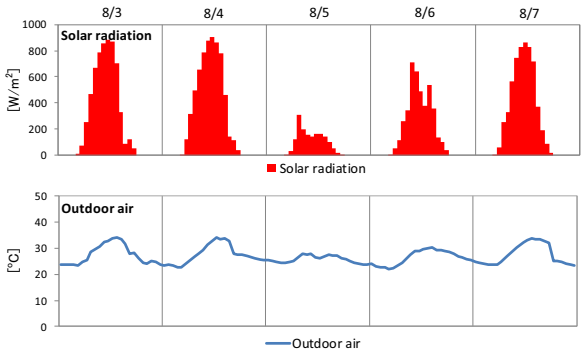

Fig. 10 Weather data on summer

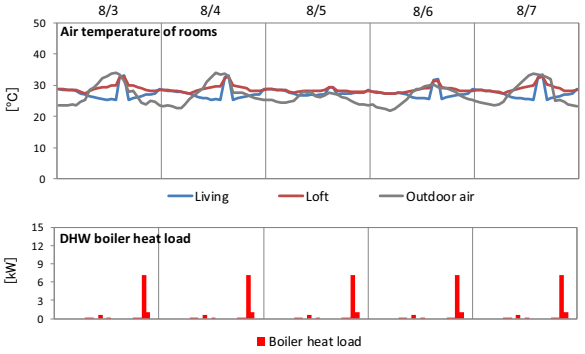

Fig. 11 simulation results of Case1

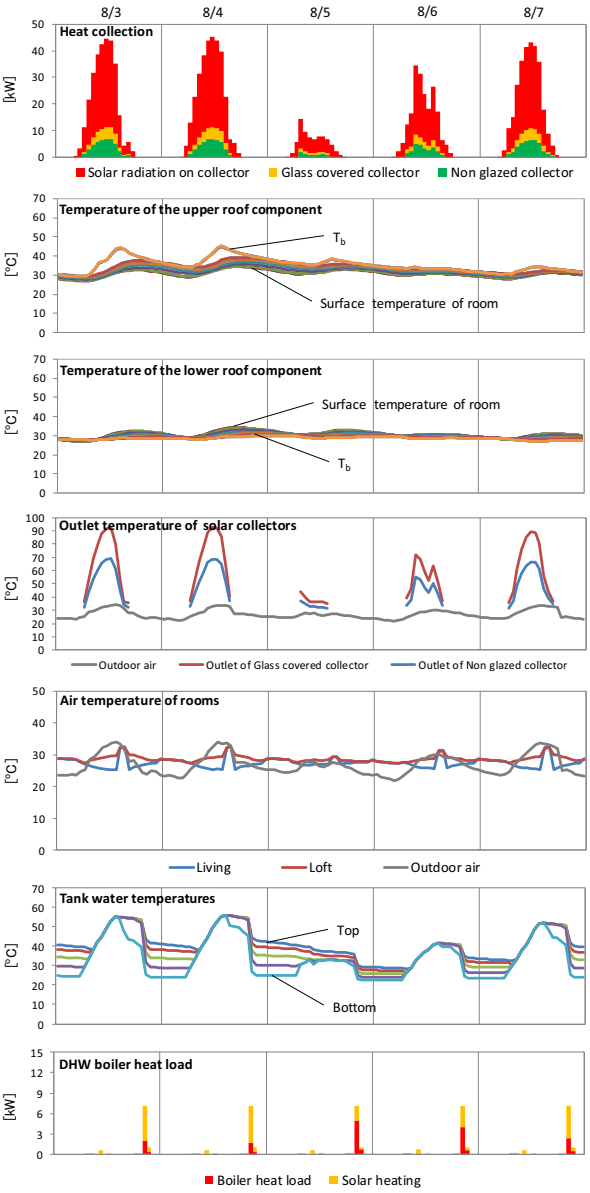

Fig. 12 simulation results of Case2 (Non glazed collector)

Fig.10 shows the weather data in the summer typical days. Figs.11, 12, 13 and 14 show the simulation results in the typical summer days. The solar radiation in Case 2 and 4 reached about 40kW on the sunny day for 48.5m^2 of the collector area. The solar radiation in Case3 reached about 15kW on the sunny day for 16.2m^2 of the collector area. The heat collection in Cases 2 and 4 reached about 10kW as the total of the upper roof collector and the lower roof collector. The heat collection in Case 3 was about 5kW. The heat collection had no large difference with the winter.

The power generation slightly increased compared to the winter. The surface temperature of PV in Cases 3 and 4 reached about 60^{o}C. The boundary temperature in Cases 2 and 4 reached about 40^{o}C. However, in Cases 2 and 4 the roof was well insulated, the influence was small for the room. The lower roof outlet air temperature in Cases 2 and 4 reached about 60^{o}C. The upper roof outlet air temperature in Cases 2 and 4 reached about 80^{o}C. The upper roof outlet air temperature in Case 3 was about 70^{o}C. The tank water temperatures in Cases 2 and 4 reached about 60^{o}C. The tank water temperature in Case 3 was about 50^{o}C. For the domestic hot water heating in Cases 2 and 4 about 80% was provided by the solar energy on the sunny day. The about 60% of the domestic hot water heat load in Case 3 was provided by the solar energy on the sunny day.

5. Annual simulation results

Tab. 5 shows the annual simulation results. Fig. 15 shows the annual simulation results. In Case 1, the heating load was 1250kWh. In Case 2, the heating load was 335kWh. In Case 2 the auxiliary heating load was reduced by 73% compared with Case 1.

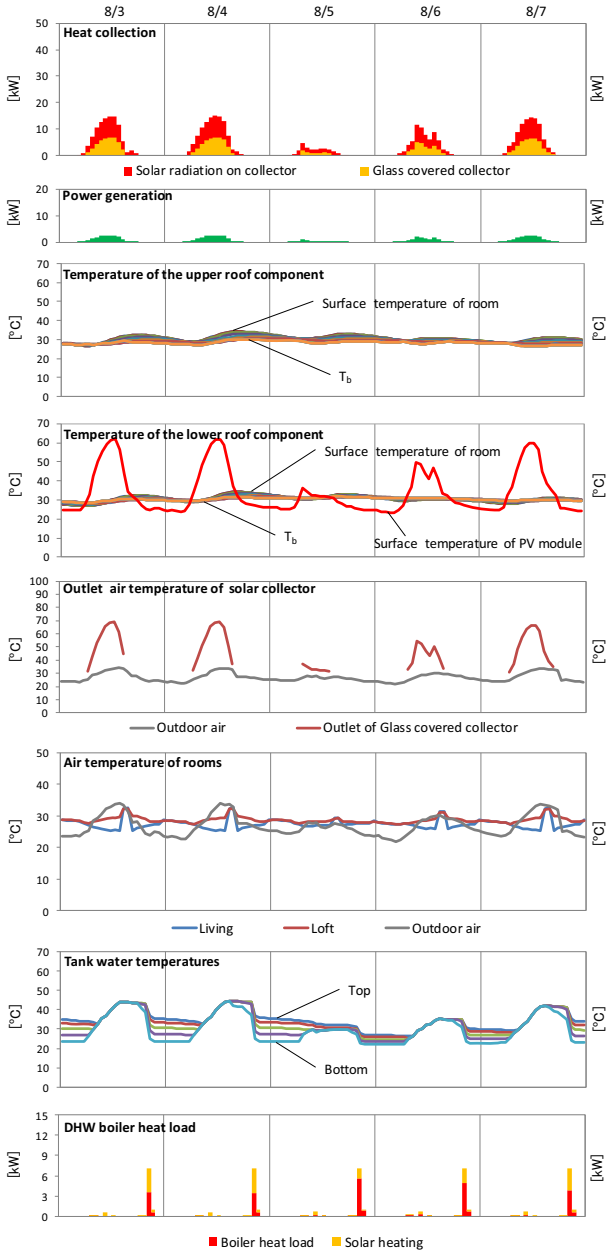

Fig. 13 simulation results of Case3 (PV module without pre-heat collector)

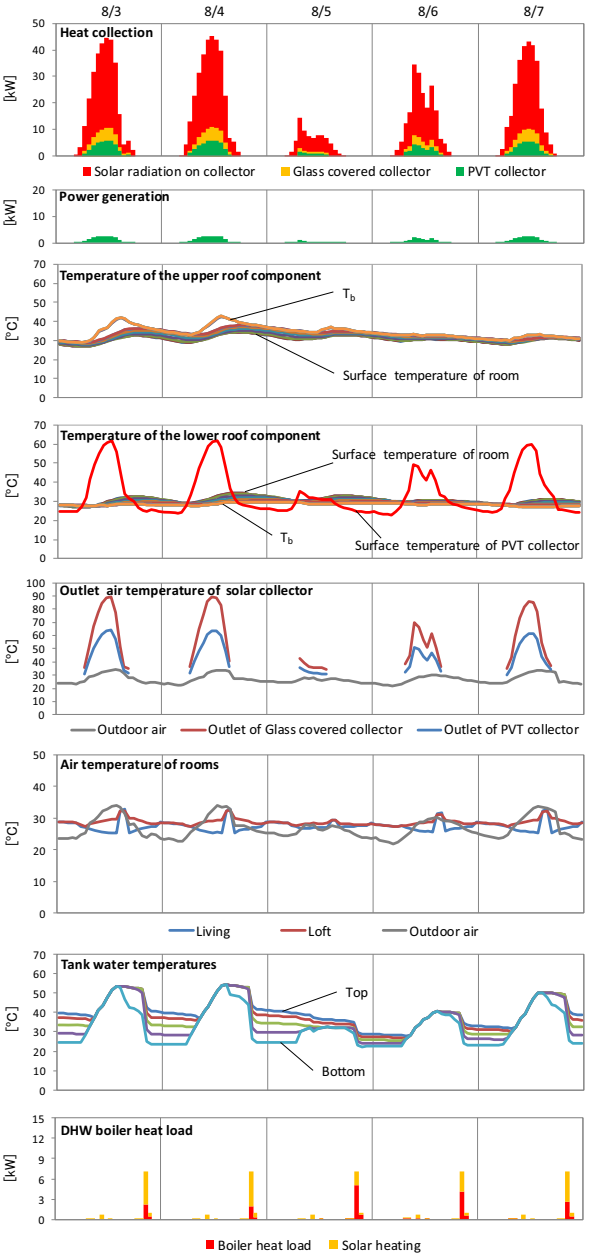

Fig. 14 simulation results of Case4 (PVT collector)

In Case 3, the heating load was 639kWh. Because, Case 3 had not the preheat collector, the reduction of the auxiliary heating load was 49% against that in Case 1 In Case 4, the heating load was 368kWh. About 71% of the auxiliary heating load was reduced against Case 1.In Case 1, the domestic hot water heating load was 4908kWh. In Case 2, the domestic hot water heating load was 3612kWh. In Case2 the domestic hot water heating load reduced by 26% compared with Case 1. In Case 3, the domestic hot water heating load was 4200kWh. In Case 3 the domestic hot water heating load reduced by 14% compared with Case 1. In Case 4, the domestic hot water heating load was 3702kWh. In Case 4 the domestic hot water heating load reduced by 24% compared with Case 1. In Case3, the PV power generation was 4674kWh. In Case4, the PV power generation becomes 4693kWh and the PV power generation of Case 4 was slightly higher than that of Case 3. The PV power generation efficiency was slightly improved for the lower temperature of the PV module by the backside ventilation.

Tab. 6 Annual simulation results

			Case1	Case2	Case3	Case4
Lower roof collector			-	Non glazed collector	PV modules	PVT collector
Upper roof collector			-	Glass covered collector		
Heat loads	Heating	[kWh]	1250	335	639	368
	DHW heating	[kWh]	4908	3612	4200	3702
	Cooling	[kWh]	1726	1703	1674	1709
Power generation		[kWh]	-	-	4674	4693

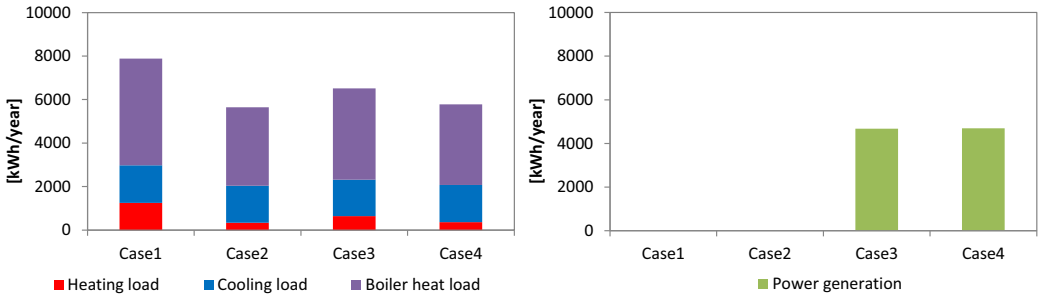

Fig. 15 Annual simulation results

6. Conclusion

The simulation of a whole solar heating system with the integrated solar collectors with PV modules was carried out to evaluate the solar heat collection, the generated electricity by PV modules, reduction of space heating and domestic hot water heating loads.

1) Case 2 using the pre-heat collector and the glass covered collector was the best for the reduction of the space heating load and domestic hot water heating load. However, Case 4 using the PVT collector for the pre-heat is the most efficient, considering the PV power generation.

2) The power generation efficiency of Case 4 with the backside ventilation was slightly higher than that in Case 3 without backside ventilation inside surface of the roof integrating the collector. However, there was no significant difference.

3) The significant effect was not found on the indoor thermal environment by the temperature rise of the inside surface of the roof integrating the collector.

References

K. Oba, M. Udagawa, A. Narita, K. Hirayanagi, Y. Matoba, T. Kusunoki, H. Roh, 2011, Predicted performance of renovated solar hoses using air collecters Part.3 T House in Takasaki, Architecture Institute of Japan, D-2, 233-234. (in Japanese)

Y.Matoba, M. Udagawa, T. Kusunoki, K.Hirayanagi, 2010, Simulation of the roof integrated solar collectors

Part.2 Air heating collectors, JSES/JWEA Joint Conference, 367-370. (in Japanese)

K. Hirayanagi, M. Udagawa, T. Kusunoki, Y. Matoba, 2011, Simulation study on the solar house with roof integrated air collector, The Society of Heating, Air Conditioning and Sanitary Engineers of Japan. (in Japanese)

AIJ (Architectuaral Institute of Japan), 2005, Expended AMeDAS Weather Date (in Japanese)

Duffie J.A, Deckman W.A, Solar Engineering of Thermal Processes, 1980 Wiley-Interscience.

M. Udagawa, M. Satoh, 1999, Energy Simulation of Residential Houses Using EESLISM. Proceedings of Sixth International IBPSA Conference, Kyoto, Japan, 91-98.